LARGE PRIMTIVE ASTEROIDS: DYNAMICAL AND THERMAL CONTEXT. D. Takir[1], W. Neumann[2], J.P. Emery[3]. [1]JETS/ARES, NASA JSC, Houston, TX (driss.takir@nasa.gov), [2]German Aerospace Center, Institute of Planetary Research, Berlin, Germany, [3]Northern Arizona University, Flagstaff, AZ.

Introduction: Primitive asteroids are important because they provide information related to the abundance and distribution of minerals and chemical compounds in the early solar system and the conditions in which the solar nebula was formed. The study of these asteroids allows us then to better constraint the current dynamical and thermal theories of the formation and evolution of the early solar system. [1,2] studied 40 primitive asteroids in the outer Main Belt region that led to the identification and distribution of at least four spectral groups, each of which is presumably related to distinct surface mineralogy. The groups were classified based on the 3-μm band (a spectral region that includes H_2O/OH absorptions). The first group (sharp) exhibits a characteristically sharp 3-μm feature, attributed to v_1 symmetric HOH and v_3 asymmetric OH stretch in phyllosilicates. The majority of asteroids in this group are concentrated in the 2.5 < a < 3.3 AU region. The second group (rounded) exhibits a rounded 3-μm feature possibly attributed to H_2O ice, is concentrated in the 3.4 < a < 4.0 AU region. The third group, Europa-like, has a 3-μm band centered at ~3.15 μm with longer wavelength band minimum and steeper rise on the long-wavelength edge of the absorption. The fourth group, Ceres-like, is located in the 3.4-4.0 AU region and has a narrow 3-μm band center at ~3.05 μm superposed on a much wider absorption from ~2.8 to 3.7 μm. Here we present additional primitive asteroids observed using the NASA Infrared Telescope Facility (IRTF), increasing our sample size of primitive asteroids to 80 objects. The main focus of this talk will be on the large primitive asteroids, Europa-like and Ceres-like groups (groups 3 and 4).

Observations and data reduction: The additional primitive asteroids were observe with the long-wavelength cross-dispersed (LXD: 1.9- 4.2 μm) mode of the SpeX spectrograph/imager at IRTF [3]. We obtained LXD data of asteroids over the course of many periods between 2015 and 2019. We used the IDL (Interactive Data Language)-based spectral reduction tool Spextool (v4.0) [4] to reduce the data. OH-line emission dominates the background sky through most of the wavelength range while thermal emission from the sky and telescope is significant longward of ~2.3 μm. Hence, to correct for these contributions, we subtracted spectra of asteroids and their corresponding standard stars at beam position A from spectra at beam B. We extracted spectra by summing the flux at each channel within a user-defined aperture. We conducted wavelength calibration at λ > 2.5 μm using telluric absorption lines. We removed the thermal excess in asteroids' spectra using the methodology described in [5] and references therein. To constrain asteroids' model thermal flux, we fitted the measured thermal excess with a model thermal excess. Then, we subtracted this model thermal flux from the measured relative spectra of asteroids. To calculate the thermal flux in the 3-μm region, we used the Near-Earth Asteroid Thermal Model (NEATM) [6], which is based on the Standard Thermal Model (STM) of [7].

Results: Most of the observed primitive asteroids were found to exhibit a characteristically sharp 3-μm feature attributed to OH-stretching in hydrated minerals (e.g., phyllosilicate). The majority of asteroids in this group are concentrated in the 2.5 < a < 3.3 AU region. We also identified three new additional asteroids with Europa-like 3-μm feature: 372 Palma, (259) Aletheia, and 87 Sylvia (**Fig. 1**). These new asteroids along with the already-observed Ceres- and Europa-like group members are localized in the ~2.8 < a < ~3.5 AU region and characterized by larger sizes **(Fig. 2).**

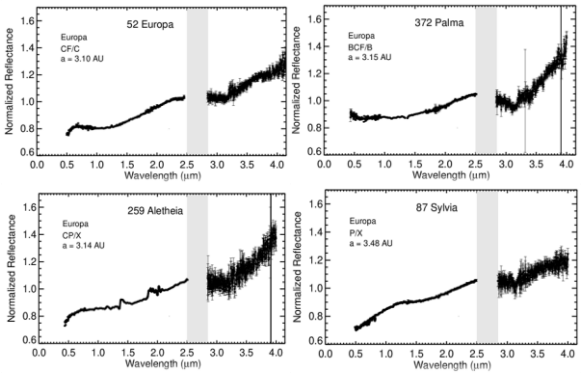

Figure 1. *Spectra (~0.5-4-μm) of asteroids 372 Palma, 259 Aletheia and 87 Sylvia with a 3-μm band similar to asteroid (52) Europa (Europa-like group)..*

Orbital distribution of large primitive asteroids: Europa- and Ceres-like groups, which include the largest asteroids in the solar system, show an interesting orbital distribution. These groups two are located in the 2.6 < a < 3.6 AU region that contains the snow-line (**Fig. 2**). The snow-line's location may have been drifted inwards due to the disk's cooling and evolution [8, 9]. Recent dynamical models (e.g., [10, 11]) suggested that a substantial fraction of primitive asteroids originated between or beyond the giant planets (a > 5 AU), where water ice would have been stable, and then implanted in the outer Main Belt space as a consequence of the giant planets' growth.

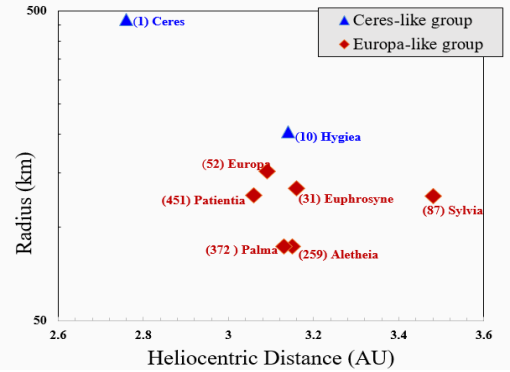

Figure 2. *Orbital distribution of Europa-like and Ceres-like group.*

Thermal modeling and evolution of primitive asteroids: Primitive water-rich asteroids are thought to be originally composed of mixtures of anhydrous materials and water ice that was later melted by heating sources such as the decay of ^{26}Al, reacting with anhydrous materials to form H_2O/OH-rich minerals. Calculations of the evolution of the temperature and structure of icy planetesimals were performed using a 1D finite differences thermal evolution model [12, 13] for ^{26}Al-heated planetesimals. In particular, thermally activated compaction due to hot pressing of bodies with an initially unconsolidated porous structure is included. An ice-rich initial composition that leads to a material dominated by phyllosilicates upon aqueous alteration (with 25 vol% H_2O and a rock fraction that contains 85 vol% phyllosilicates and 15 vol% olivine upon aqueous alteration, similar to CI and CM chondrites) was assumed. A typical initial porosity of 40% [14] is reduced following the change of the strain rate that is calculated as Voigt approximation from the strain rates of components [15]. Material properties (thermal conductivity, density, heat capacity, etc.) correspond to the composition assumed and are adjusted with temperature and porosity. Melting of the water ice as well as water-rock separation are included [13]. Both short- and long-lived radionuclides are considered as heat sources. **Fig. 3** shows the maximum temperature calculated as a function of radius and accretion time. A variety of internal structures is obtained, ranging from primordial (no melting of water ice) over partially melted or partially differentiated (melting of water ice, hydration, formation of a rocky core and water ocean below an undifferentiated layer) to completely differentiated ones (rocky core, water mantle, Enceladus-like case).

The heating and differentiation of planetesimals is determined by the availability of ^{26}Al, i.e., by the accretion time t_0 relative to the formation of the calcium-aluminum-rich inclusions (CAIs), such that maximum temperatures and structures vary strongly for $t_0 < 6$ Myr rel. to CAIs. However, for a later accretion only the size of the body determines its maximum temperature and structure due to the nearly constant heating by long-lived radionuclides. Average densities of Ceres- and Europa-like group members imply highly porous interiors and, consequently, relatively late accretion at $t_0 > 3$ Myr rel. to CAIs with a maximum temperature of < 600 K (**Fig. 3**).

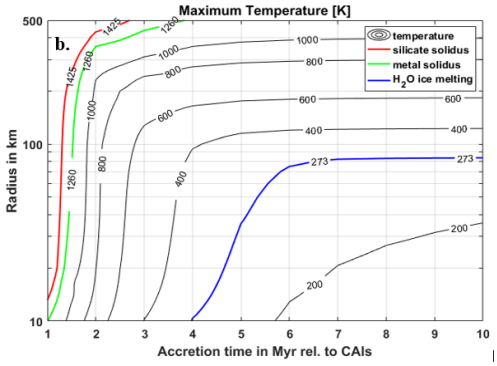

Figure 3. *Maximum temperature for icy planetesimals as a function of the accretion time rel. to CAIs and of the radius.*

References: [1] Takir D. and Emery J.P. (2012) *Icarus*, 219, 641-654. [2] Takir et al. D. (2015) *Icarus*, 257, 185-193. [3] Rayner J.T. (2003) *ASP* 155, 362-382. [4] Cushing M.C. (2004) *ASP*, 166, 362-376. [5] Rivkin A.S. et al. (2003) MAPS 38, 1383–1398. [6] Harris A.W. (1998) Icarus, 131, 291-301. [7] Lebofsky et al. L.A. (1986) Icarus 68, 239-251. [8] Cyr K.E. et al. (1998) Icarus 135, 537-548. [9] Dodson-Robinson S.E. et al. (2009) Icarus 200, 672–693. [10] Walsh K.J. et al. (2013) Nature 475, 206-209. [11] Raymond and Izodoro (2017) Icarus, 297, 134-148. [12] Neumann W. et al. (2015) A&A, 584, A117. [13] Neumann W. et al. (2020) A&A, doi: https://doi.org/10.1051/0004-6361/201936607, in press. [14] Henke et al. (2012) A&A, 537, A45. [15] Dygert N. et al. (2016) GRL, 43, 532.

Acknowledgements: Part of this research is funded by NASA Solar System Observations Program grant NNX17AJ24G (PI: Driss Takir). NASA IRTF is operated by the University of Hawai'i under contract NNH14CK55B with NASA.